CRA-024781: a novel synthetic inhibitor of histone deacetylase enzymes with antitumor activity *in vitro* and *in vivo*

Joseph J. Buggy, Z. Alexander Cao, Kathryn E. Bass, Erik Verner, Sriram Balasubramanian, Liang Liu, Brian E. Schultz, Peter R. Young, and Stacie A. Dalrymple

Celera Genomics, South San Francisco, California

Abstract

CRA-024781 is a novel, broad spectrum hydroxamic acid–based inhibitor of histone deacetylase (HDAC) that shows antitumor activity *in vitro* and *in vivo* preclinically and is under evaluation in phase I clinical trials for cancer. CRA-024781 inhibited pure recombinant HDAC1 with a K_i of 0.007 μmol/L, and also inhibited the other HDAC isozymes HDAC2, HDAC3/SMRT, HDAC6, HDAC8, and HDAC10 in the nanomolar range. Treatment of cultured tumor cell lines grown *in vitro* with CRA-024781 resulted in the accumulation of acetylated histone and acetylated tubulin, resulting in an inhibition of tumor cell growth and the induction of apoptosis. CRA-024781 parenterally administered to mice harboring HCT116 or DLD-1 colon tumor xenografts resulted in a statistically significant reduction in tumor growth at doses that were well tolerated as measured by body weight. Inhibition of tumor growth was accompanied by an increase in the acetylation of α-tubulin in peripheral blood mononuclear cells, and an alteration in the expression of many genes in the tumors, including several involved in apoptosis and cell growth. These results reveal CRA-024781 to be a novel HDAC inhibitor with potent antitumor activity. [Mol Cancer Ther 2006;5(5):1309–17]

Introduction

The acetylation of lysine residues on the amino terminal tails of nucleosomal histone proteins has a crucial role in the regulation of the chromatin structure. The acetylation state of histones is maintained by the opposing actions of histone acetyl transferase enzymes and histone deacetylases (HDAC). There are 11 known isoforms of the classic HDAC family, denoted HDAC1 to HDAC11 (1, 2). In addition to histones, HDAC enzymes are known to deacetylate other proteins, including α-tubulin (3), suggesting complex, multifunctional roles for HDACs *in vivo*.

One of the best studied roles of HDAC enzymes is their ability to function as transcriptional corepressors. HDAC enzymes are recruited to specific promoters to repress transcription by deacetylating histones proximal to the promoter. Histone deacetylation is thought to repress transcription by increasing the affinity of histones for DNA, thereby sterically preventing access of transcription factors to promoter regions. Inhibitors of HDAC enzymes have been shown to alter the expression of ~2% to 10% of transcribed genes in the human genome. Interestingly, these changes include genes both strongly up-regulated and down-regulated, suggesting that the role of HDAC enzymes is more complex than simple corepression. Genes up-regulated by HDAC inhibitors include the tumor suppressor $p21^{Cip1/WAF1}$, p16, gelsolin, histones, and caspases, whereas down-regulated genes include Her2/neu, vascular endothelial growth factor, and cyclin proteins (4).

Alterations in the acetylation state of specific lysines have been associated with human cancer (5). It has been hypothesized that aberrant patterns of histone acetylation function to maintain the transformed state of human tumors, a state that can be reversed by inhibiting HDAC enzymes. Several studies have shown that the treatment of tumor cells with HDAC inhibitors results in growth arrest, differentiation, apoptosis, and inhibition of tumor angiogenesis (6). The precise antitumor mechanism of HDAC inhibition is unclear, and may be the result of altered transcription, or perhaps may result directly by affecting chromosome stability, assembly, or function (7, 8).

A variety of structurally distinct compounds have been described to inhibit HDAC enzymes, including hydroxamic acids, benzamides, electrophilic ketones, and cyclic peptides (9). Several hydroxamic acid–based inhibitors have been described (suberoylanilide hydroxamic acid, trichostatin A, oxamflatin, LAQ824, LBH589, and PXD101), some of which are currently in clinical trials for cancer. We have focused on the development of a hydroxamic acid–based series of compounds that has been optimized for *in vivo* efficacy and therapeutic index (10). Herein, we describe the *in vitro* and *in vivo* characteristics of a novel HDAC inhibitor, CRA-024781. CRA-024781 is currently undergoing evaluation in clinical trials for cancer.

Materials and Methods

Cell Lines

The following human tumor cell lines were obtained from the American Type Tissue Culture Collection:

Received 10/25/05; revised 2/6/06; accepted 3/2/06.

The costs of publication of this article were defrayed in part by the payment of page charges. This article must therefore be hereby marked advertisement in accordance with 18 U.S.C. Section 1734 solely to indicate this fact.

Requests for reprints: Joseph J. Buggy, Celera Genomics, 180 Kimball Way, South San Francisco, CA 94080. Phone: 650-866-6236; Fax: 650-866-6652. E-mail: drjbuggy@yahoo.com

doi:10.1158/1535-7163.MCT-05-0442

HCT116, HCT-15, BT-549, NCI-H226, CWR-22RV1, MCF-7, NCI-PC3, DLD-1, SKOV-3, and OVCAR-3. Human umbilical vein endothelial cells (HUVEC) were obtained from Cambrex (Baltimore, MD). For *in vivo* studies, HCT116 human colorectal tumor cells were cultured and expanded in McCoy's 5A medium (supplemented with 1.5 mmol/L L-glutamine and 10% fetal bovine serum), and DLD-1 human colorectal tumor cells were cultured and expanded in RPMI 1640 (supplemented with 2 mmol/L L-glutamine, 1 mmol/L sodium pyruvate, and 10% fetal bovine serum).

HDAC Activity

HDAC activity was measured using a continuous trypsin-coupled assay that has been previously described in detail (11). For inhibitor characterization, measurements were done in a reaction volume of 100 μL using 96-well assay plates. For each isozyme, the HDAC protein in reaction buffer [50 mmol/L HEPES, 100 mmol/L KCl, 0.001% Tween 20, 5% DMSO (pH 7.4), supplemented with bovine serum albumin at concentrations of 0% (HDAC1), 0.01% (HDAC2, 3, 8, and 10), or 0.05% (HDAC6)] was mixed with inhibitor at various concentrations and allowed to incubate for 15 minutes. Trypsin was added to a final concentration of 50 nmol/L, and acetyl-Gly-Ala-(*N*-acetyl-Lys)-AMC was added to a final concentration of 25 μmol/L (HDAC1, 3, and 6), 50 μmol/L (HDAC2 and 10), or 100 μmol/L (HDAC8) to initiate the reaction. Negative control reactions were done in the absence of inhibitor in replicates of eight. Reactions were monitored in a fluorescence plate reader. After a 30-minute lag time, the fluorescence was measured over a 30-minute time frame using an excitation wavelength of 355 nm and a detection wavelength of 460 nm. The increase in fluorescence with time was used as the measure of the reaction rate. Inhibition constants K_i(app) were obtained using the program BatchKi (12).

Cell Proliferation Assay

Ten tumor cell lines and HUVEC were cultured for at least two doubling times, and growth was monitored at the end of compound exposure using an Alamar blue (Biosource, Camarillo, CA) fluorometric cell proliferation assay as previously described (13). The compound was assayed in triplicate wells in 96-well plates at nine concentrations using half-log intervals ranging from 0.0015 to 10 μmol/L. The final DMSO concentration in each well was 0.15%. The concentration required to inhibit cell growth by 50% ($GI_{50\%}$) and 95% confidence intervals were estimated from nonlinear regression using a four-parameter logistic equation.

Histone and Tubulin Acetylation, $p21^{Cip1/WAF1}$ Accumulation, Poly(ADP-Ribose) Polymerase Cleavage, and Phosphorylated Histone Variant H2AX

Acetylated histone, acetylated tubulin, $p21^{Cip1/WAF1}$, poly(ADP-ribose) polymerase (PARP) cleavage, and phosphorylated histone variant H2AX (γH2AX) proteins were detected by Western blotting in cells treated with CRA-024781. Tumor cells and subconfluent HUVEC were cultured for 18 hours in the presence of CRA-024781 concentrations ranging from 0.01 to 10 μmol/L. Cells were then collected and lysed in lysis buffer (M-Per, Pierce, Rockford, IL) containing protease inhibitors (Complete, Mini, EDTA-free; Roche, Indianapolis, IN) and phosphatase inhibitors (phosphatase inhibitor cocktail set II; Calbiochem, La Jolla, CA). Lysates were solubilized in SDS-PAGE reducing sample buffer, boiled, and electrophoresed in Novex Tris-glycine gels (Invitrogen, San Diego, CA). The gels were blotted onto nitrocellulose and probed with either an antiacetyl lysine antibody (Upstate, Charlottesville, VA) to detect acetylated histone, an anti-acetylated tubulin antibody (Sigma, St. Louis, MO), an anti-$p21^{Cip1/WAF1}$ antibody (BD Biosciences, San Jose, CA), an anti-PARP antibody (Cell Signaling, Danvers, MA), or an anti-γH2AX antibody (Cell Signaling). The blots were washed, incubated with an appropriate horseradish peroxidase–conjugated secondary antibody (The Jackson Laboratory, Bar Harbor, ME) and the blots were developed for enhanced chemiluminescence (Pico Substrate Kit, Pierce).

Pharmacokinetic Analysis

CRA-024781 was formulated in 30% HP-cyclodextrin in water and a 10 mg/kg bolus dose was administered i.v. to female BALB/c *nu/nu* mice (16–22 g). Blood samples were collected over 24 hours. Plasma was prepared from each blood sample with lithium heparin and was assayed for CRA-024781 by liquid chromatography with tandem mass spectrometry. Mouse plasma samples were assayed for CRA-024781 by high-performance liquid chromatography with tandem mass spectrometric detection. Plasma samples were extracted by protein precipitation using acetonitrile (MeCN). A Hypersil C-18 column, 50 × 2.1 mm was used for sample separation. Samples were separated on reversed-phase high-performance liquid chromatography under linear gradient conditions using water/MeCN as mobile phases, at a flow rate at 0.5 mL/min. Samples were ionized under electrospray and quantified by multiple reactive monitoring, recording the transition from the molecular ion to the product ion: 398 → 200 *m/z*. Linearity (>0.25–1,000 ng/mL) was achieved with interday and intraday coefficient of variation (%) and deviation of the mean from theoretical (%) ±15%. The lower limit of quantitation was 0.25 ng/mL. Pharmacokinetic variables were estimated with compartmental methods using WinNonlin-Pro version 4.1 (Pharsight Corp., Mountain View, CA). Pharmacokinetic calculations were done using nominal doses and nominal collection times.

In vivo Efficacy Studies

Female BALB/c *nu/nu* mice were purchased from Charles River Laboratories and acclimated for 3 to 5 days prior to tumor implantation. All mice were maintained in sterilized translucent polycarbonate microisolator cages under specific pathogen–free conditions and were used in compliance with protocols approved by the Institutional Animal Care and Use Committee. HCT116 and DLD-1 tumor cells were implanted s.c. in nude mice at 3×10^6 per mouse. Tumor-bearing mice were randomized based on tumor volume prior to the initiation of treatment. Treatment with CRA-024781 started when the average tumor volume was ~100 mm^3. Tumor volume was calculated as follows: volume = $0.5 \times X^2 \times Y$, where X, tumor width; and and Y, tumor length. The vehicle used in all studies was 20% HP-β-cyclodextrin in water. Dosages were given i.v.

Compound	Structure	K_i (μM) HDAC1
CG-001	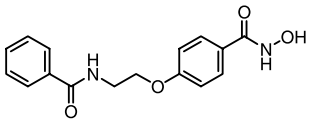	0.043
CG-002	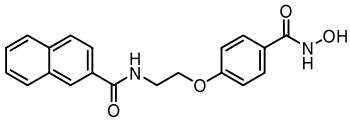	0.006
CG-003	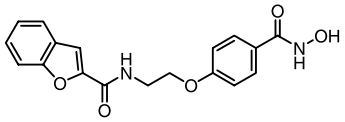	0.004
CRA-024781	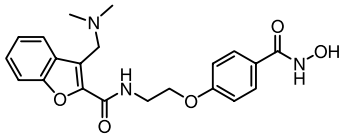	0.007
CG-004	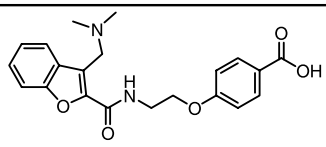	>50

Figure 1. Structure-activity relationship of HDAC inhibitors. Compound numbers, chemical structure, and inhibition constant (K_i) for HDAC1.

either every other day (q.o.d.) or for 4 consecutive days followed by 3 days without treatment for each week of the study (q.d. × 4 per week) as indicated. Inhibition of tumor growth was calculated as follows: $100 \times (1 - dT/dC)$, where dT was the change in average tumor volume since the first dose in the treatment group and dC was the change in average tumor volume since the first dose in the control group. Statistical analysis was done with one-way ANOVA on log-transformed data to meet the assumption of underlying normal distribution for the test to be valid, and *P* values were corrected for multiple comparisons to control by Dunnett's method. For single-group comparison, statistical analyses were done with *t* test on log-transformed data to meet the assumption of an underlying normal distribution for the test to be valid.

Detection of Acetylated Tubulin in Whole Blood

Blood samples collected at various time points after dosing were processed in Red Blood Cell Lysis Buffer (Roche) to isolate nucleated blood cells as per the manufacturer's instruction. Cells were pelleted and stored at −80°C until analysis. Frozen nucleated blood cell pellets were lysed in protein extraction buffer (M-Per, Pierce) containing protease inhibitors (Roche) and phosphatase inhibitors (Calbiochem). Acetylated tubulin was detected in blood lysates by Western blotting. Lysates (20 μg total protein) were solubilized in SDS-PAGE reducing sample buffer, boiled, and electrophoresed. The gels were blotted onto nitrocellulose and probed with an anti-acetylated tubulin antibody (Sigma) to detect acetylated tubulin. The blots were washed, incubated with an appropriate horseradish peroxidase–conjugated secondary antibody (The Jackson Laboratory), and the blots were developed for enhanced chemiluminescence (Pico Substrate Kit, Pierce).

Microarray Analysis

Transcriptional profiles of tumor samples were obtained on Codelink Human Uniset 1 oligonucleotide microarrays (GE-Amersham, Piscataway, NJ). Tumors from compound- and corresponding vehicle-treated tumors were lyophilized and one part of the tumor powders were used to prepare the RNA using Qiagen RNeasy kits (Qiagen, Inc., Valencia, CA). Equal amounts of RNA from at least three animals per dose/drug/time point were pooled together for analysis. Biotin-labeled cRNA probes were prepared from the total RNA by standard GE-Codelink IVT protocols. Ten micrograms of biotinylated cRNA were fragmented and hybridized to the arrays. Arrays were hybridized for 18 hours at 37°C, washed and detected with Strepatavidin-Alexa 647 (Codelink protocol v2.1). They were scanned with an Axon GenePix 4000B scanner (Axon Instruments, Union City, CA) and the images were processed with Codelink 4.0 batch processing software. The data were then transferred to a Signet database and analyzed in Genespring (Agilent, Inc., Palo Alto, CA). Only genes flagged as ''good'' by the Codelink quality control software were used in the analyses. Each treated sample was normalized to the corresponding vehicle control.

TaqMan Analysis

TaqMan gene expression assays for selected genes were obtained from Applied Biosystems, Inc. One-step reverse transcription-PCR was carried out in triplicate on 25 ng of total RNA from each sample on an ABI PRISM 7700 instrument according to standard protocols. The mRNA levels for each gene were normalized to the amount of RNA in the well as measured in parallel using Ribogreen (Invitrogen). The treated samples were then normalized to the vehicle control at that time point.

Results

Chemical Design and Synthesis

In our efforts to design and develop small-molecule inhibitors of HDACs, we identified a promising

Table 1. CRA-024781 inhibits multiple HDAC isoforms

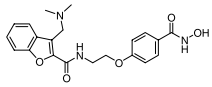

Isoform	K_i (μmol/L) ± SD
HDAC1	0.007 ± 0.001
HDAC2	0.019 ± 0.002
HDAC3/SMRT	0.0082 ± 0.001
HDAC6	0.017 ± 0.002
HDAC8	0.28 ± 0.05
HDAC10	0.024 ± 0.019

Table 2. CRA-024781 inhibits the growth of tumor cell lines

Cell line	Origin	T_d (h)*	Assay (h)	$GI_{50\%}$ (μmol/L), 95% confidence interval†
HCT-116	Colon	14	48	0.20 (0.14-0.26)
DLD-1	Colon	22	48	0.53 (0.41-0.64)
HCT-15	Colon	22	48	1.59 (1.18-1.99)
MCF-7	Breast	37	96	0.15 (0.10-0.20)
BT-549	Breast	29	72	3.09 (1.75-4.42)
NCI-H226	Lung	25.4	72	1.45 (0.96-1.93)
CWR-22RV1	Prostate	30.4	96	0.15 (0.12-0.18)
NCI-PC3	Prostate	18.8	48	0.38 (0.33-0.43)
SKOV-3	Ovary	44.4	120	0.65 (0.59-0.71)
OVCAR-3	Ovary	46	120	0.16 (0.14-0.18)
HUVEC	Endothelium	15	48	0.43 (0.15-0.71)

NOTE: Growth inhibition of human tumor cell lines and HUVEC by CRA-024781.
*T_d, doubling time.
†The $GI_{50\%}$ data are estimated from nonlinear regression using a four-parameter logistic equation from single experiments, with the exception of HCT 116 cells, which were tested four times.

N-hydroxy-benzamide lead series (Fig. 1). Design and synthesis led to the benzofuran amide analogues exemplified by CG-003 (K_i HDAC1 = 0.004 μmol/L) and further optimization of this series for *in vivo* efficacy and pharmacokinetics provided our lead inhibitor CRA-024781 (K_i HDAC1 = 0.007 μmol/L). The hydroxamic acid functionality was essential for potency because replacement with a carboxylic acid led to an inactive compound, as seen with CG-004 (K_i HDAC1 > 50 μmol/L). CRA-024781, a compound chosen for further preclinical development, inhibited purified recombinant HDAC isoforms in the nanomolar range as shown in Table 1. Inhibition constants ranged from 0.007 (HDAC1) to 0.28 μmol/L (HDAC8).

Effect on Tumor Cell Proliferation

In order to determine if HDAC inhibition by CRA-024781 affects the proliferation of tumor cells, a panel of human tumor cell lines was treated *in vitro* with various concentrations of inhibitor. Cells were treated with CRA-024781 for durations based on the intrinsic doubling times of each tumor cell line, and these data were used to calculate a $GI_{50\%}$ value as shown in Table 2. Antitumor activity was observed in all 10 tumor cell lines tested, with $GI_{50\%}$ values ranging from 0.15 to 3.09 μmol/L. In addition, CRA-024781 had an antiproliferative effect on HUVEC endothelial cells with a $GI_{50\%}$ value of 0.43 μmol/L. Based on these data, we decided to focus on the further characterization of the effects of CRA-024781 in two colon tumor cell lines, HCT116 ($GI_{50\%}$ = 0.2 μmol/L) and DLD-1 ($GI_{50\%}$ = 0.53 μmol/L).

Effect on Protein Acetylation, $p21^{Cip1/WAF1}$ Induction, and the Apoptosis Markers PARP and γH2AX

We further characterized the antitumor mechanism of CRA-024781 by treating both HCT116 and DLD-1 colon tumor cells with increasing concentrations of compound and measuring the accumulation of various mechanistic biomarkers proposed to be involved in the antitumor activity of HDAC inhibitors. Treating either HCT116 or DLD-1 cells with CRA-024781 resulted in the dose-dependent accumulation of both acetylated histones and acetylated tubulin (Fig. 2A and B) suggesting that HDAC enzymes are inhibited in these cells. In addition, CRA-024781 induced expression of the cyclin-dependent kinase inhibitor, $p21^{Cip1/WAF1}$, a protein postulated to play a role in the antitumor effect of HDAC inhibition (14). In order to determine if CRA-024781 treatment of these tumor lines led to apoptosis, PARP cleavage and the accumulation of the γH2AX were assayed after compound incubation for 18 hours. γH2AX formation is an early chromatin modification that occurs following initiation of DNA fragmentation during apoptosis (15). PARP cleavage and γH2AX were detected in both cell lines in the low micromolar range. Interestingly, treatment of HUVEC cells showed no accumulation of PARP or γH2AX, suggesting that these endothelial cells do not undergo apoptosis following treatment with CRA-024781 for 18 hours (Fig. 2C). The appearance of the acetylated histone and tubulin biomarkers roughly tracked with the differential sensitivity of HCT116 and DLD-1 to growth inhibition by CRA-024781.

In vivo Pharmacokinetics

Having established that CRA-024781 displayed HDAC inhibitory and antitumor properties *in vitro*, we assessed the pharmacokinetics of the compound to evaluate exposure in order to enable further testing in efficacy models. CRA-024781 was delivered i.v. to female mice and plasma concentrations were monitored over time (Fig. 3). Based on these data, the clearance was calculated to be 297 mL/min/kg, the volume of distribution in the central compartment was 3,750 mL/kg, the steady-state volume of distribution was 9,230 mL/kg, the predominant plasma half-life was 6.7 minutes (73% area under the curve), and the mean residence time was 31 minutes. These data suggest that CRA-024781 had sufficient *in vivo* exposure when given by the i.v. route of administration for use in the study of the biological effects of HDAC inhibition *in vivo*.

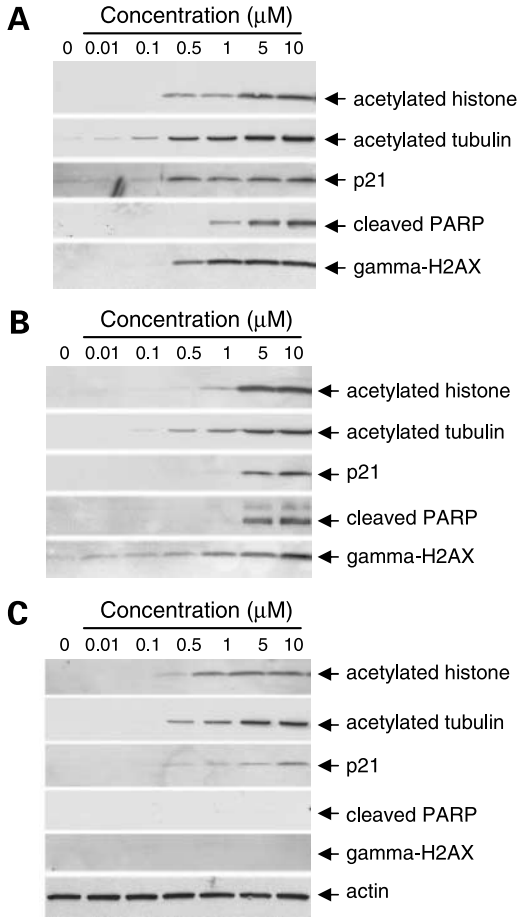

Figure 2. CRA-024781 activates biomarkers of HDAC inhibition. Accumulation of acetylated histone, acetylated tubulin, $p21^{Cip1/WAF1}$, cleaved PARP, and γH2AX are detected by Western blotting of lysates from treated HCT116 (**A**) and DLD-1 (**B**) cells. **C,** HUVEC cells.

Antitumor Activity and Induction of Acetylation by CRA 024781 *In vivo*

In order to assess the antitumor activity of CRA-024781 *in vivo*, mice bearing human colon tumor xenografts were dosed i.v. with the compound using various dosages and schedules. I.v. administration of CRA-024781 in a previous dose scheduling study in HCT116 xenografts identified two regimens with good therapeutic indices: (*a*) once daily every other day (q.o.d.) or (*b*) once daily for 4 consecutive days followed by 3 days without treatment each week (q.d. × 4 per week; dose scheduling data not shown). When CRA-024781 was evaluated in HCT116 or DLD-1 xenografts according to the first regimen at a dosage of 200 mg/kg i.v. q.o.d., statistically significant inhibition of tumor growth was observed (Fig. 4A and B). The inhibition of tumor growth was 69% ($P < 0.000001$) and 59% ($P < 0.01$) for HCT116 and DLD-1 models, respectively. Although some body weight loss approaching 13% relative to vehicle controls was observed in the DLD-1 study, no body weight loss was observed in the HCT116 study, suggesting that there was some tolerability variation across experiments, and that 200 mg/kg was near the maximum tolerated dose for q.o.d. administration (data not shown). CRA-024781 was then evaluated at multiple doses using the second regimen (q.d. × 4 per week). In the HCT116 model, inhibition of tumor growth was 48% ($P < 0.05$), 57% ($P < 0.01$), 82.2% ($P < 0.0001$), and 80.0% ($P < 0.0001$) for 20, 40, 80, and 160 mg/kg, respectively. None of these doses led to reductions in animal weight relative to vehicle by the end of the study (data not shown). In the DLD-1 model, CRA-024781 administered q.d. × 4 per week did not significantly inhibit tumor growth, although a marginally significant trend towards inhibition was observed with the highest dose of 160 mg/kg, showing 43% inhibition ($P = 0.09$) with no associated body weight loss (data not shown). In order to determine if the plasma concentrations of CRA-024781 attained in the studies were sufficient to inhibit HDAC enzymes *in vivo*, peripheral blood cells were examined *ex vivo*. As shown in Fig. 5, each treatment group had a measurable increase in tubulin acetylation at 2 and 6 hours after dosing. In summary, CRA-024781 exhibited statistically significant antitumor activity against both HCT116 and DLD-1 human colorectal tumor xenografts, although antitumor activity overall seemed to be more pronounced in the HCT116 xenograft model.

Transcriptional Profile of CRA-024781

To gain insights into the mechanism by which CRA-024781 inhibits tumor growth, mRNA profiles of HCT-116 and DLD-1 tumors were compared from animals treated with CRA-024781 at efficacious doses (80 and 160 mg/kg for HCT-116, and 160 mg/kg for DLD-1), and at different times (from 2 to 48 hours) using microarray analysis. Hierarchical clustering was done on the microarray data using the standard correlation algorithm in GeneSpring as shown in Fig. 6. Expression changes were seen in ~15% of all expressed genes (990 genes out of the 6,640 total genes that passed quality control criteria). In general, maximal

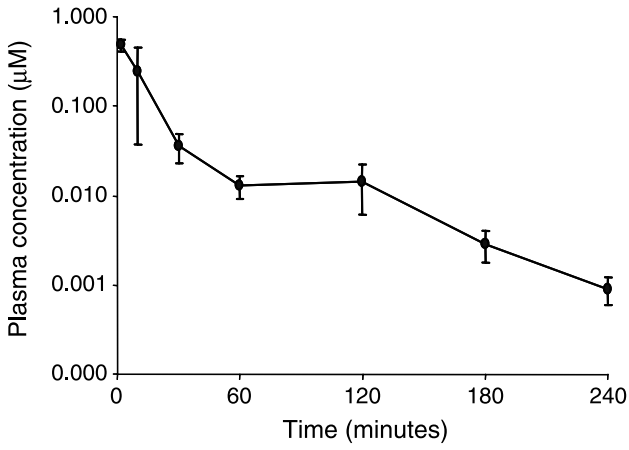

Figure 3. Pharmacokinetics of CRA-024781. Plasma concentration versus time following i.v. administration at 10 mg/kg in female BALB/c nude mice ($n = 3$/time point).

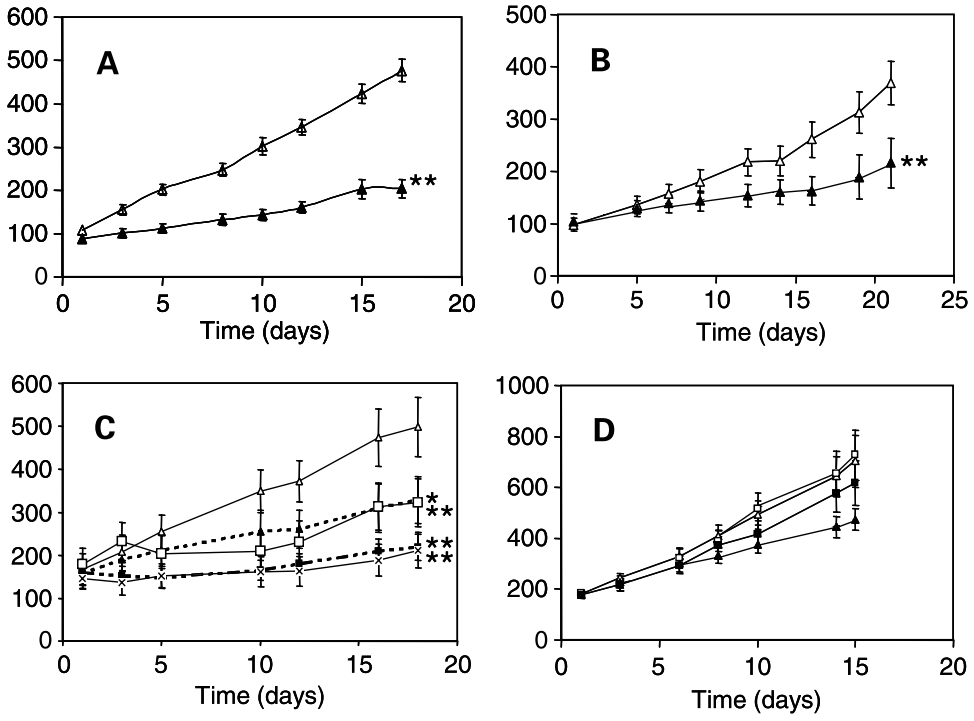

Figure 4. CRA-024781 inhibits the growth of human tumor xenografts *in vivo*. The growth of tumors over time is plotted in **A:** HCT116 colon tumor xenograft model [vehicle alone (△), 200 mg/kg (▲); schedule, q.o.d.]. **B,** DLD-1 colon tumor xenograft model [vehicle alone (△), 200 mg/kg (▲); schedule, q.o.d.]. **C,** HCT116 colon tumor xenograft model [vehicle alone (△), 20 mg/kg (▲) 40 mg/kg (□) 80 mg/kg (■) 160 mg/kg (×); schedule, q.d. × 4]. **D,** DLD-1 colon tumor xenograft model [vehicle alone (△), 60 mg/kg (■), 100 mg/kg (□), 160 mg/kg (▲); schedule, q.d. × 4]. *, $P < 0.05$; **, $P < 0.01$; *bars,* calculated as described in Materials and Methods.

differential expression was seen at 2 and 4 hours, and more minimal changes occurred at the 24-hour and 48-hour time points, consistent with both the pharmacokinetics and with the tubulin acetylation data. A pattern of up-regulated genes was observed at some early time points (Fig. 6, *red box*) and another pattern of down-regulated genes were found at the mid (4- to 6-hour) time points (*yellow box*). Interestingly, this pattern of down-regulated genes was also seen at the 2-hour time point of the highest (160 mg/kg) dose in HCT-116 tumors. A subset of these differentially expressed genes is shown in Table 3. Genes were selected that met a statistical filter of $P < 0.05$, represented a >1.8-fold change in gene expression averaged from both the early (2-hour) and mid (4- to 6-hour) time points.

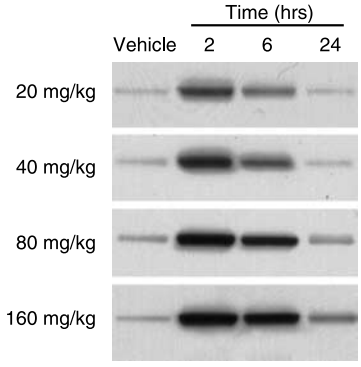

Figure 5. *In vivo* pharmacodynamics of CRA-024781. Peripheral blood mononuclear cells were prepared from blood drawn at the time points indicated from mice dosed in the HCT116 efficacy study shown in Fig. 4C. Acetylation of α-tubulin was detected by Western blot.

Discussion

Herein, we have described CRA-024781, a novel hydroxamic acid–based inhibitor of HDAC enzymes with potent antitumor activity *in vitro* and *in vivo*. This compound was derived from a series of compounds designed around an *N*-hydroxy-benzamide scaffold, and was optimized for potency against HDAC enzymes and for *in vivo* antitumor activity. CRA-024781 inhibited all of the HDACs tested with K_i values ranging from 0.007 to 0.28 μmol/L.

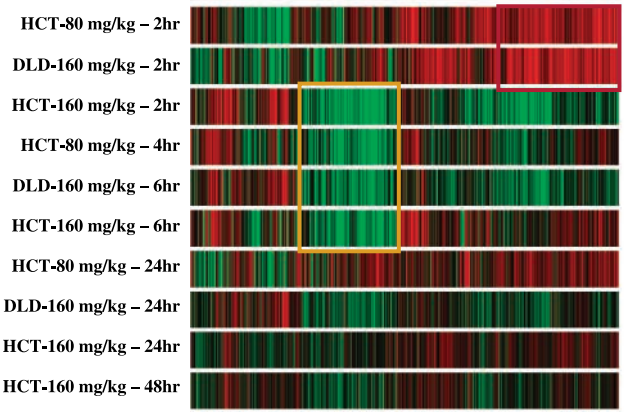

Figure 6. Effect of CRA-024781 on gene expression. A hierarchical clustering analysis of tumors from mice treated with CRA-024781. *Red,* genes up-regulated >1.8-fold; *green,* genes down-regulated >1.8-fold; *black,* others. Each column corresponds to a CRA-024781-treated sample which was normalized to its corresponding vehicle treatment at the same time point. Clusters of similarly up-regulated (*red box*) or down-regulated (*yellow box*) genes.

Table 3. Genes affected by CRA-024781 in tumor xenografts grown *in vivo*

Symbol	Gene name	Biological process	GenBank accession no.	Fold change
Up-regulated genes				
RGL1	Ral GDS-like gene	Signal transduction	NM_015149	4.3
DHRS2	Dehydrogenase/reductase member 2	Oxidation and reduction	NM_005794	3.8
GCDH	Glutaryl-CoA dehydrogenase	Lipid and fatty acid metabolism	NM_013976	3.0
CTGF	Connective tissue growth factor	Oncogenesis; signal transduction	NM_001901	2.6
FUCA1	Fucosidase	Protein modification	NM_000147	2.6
SERPINE1	Serine protease inhibitor 1 (PAI-1)	Blood clotting	NM_000602	2.4
TNFRSF17	BCM	Immunity and defense	NM_001192	2.4
RBBP5	Retinoblastoma binding protein 5	Cell proliferation	NM_005057	2.3
CDKN1A	Cyclin-dependent kinase inhibitor (p21)	Cell cycle	NM_000389	2.3
SIRT4	Sirtuin 4	DNA binding and metabolism	NM_012240	2.2
FYN	Fyn oncogene	Oncogenesis; signal transduction	AA682448	2.2
H2AFL	H2A histone family member L	DNA binding and metabolism	NM_003512	2.0
CASP3	Caspase 3	Apoptosis	NM_032991	1.9
CASP1	Caspase 1	Apoptosis	NM_033292	1.8
CDKN2D	Cyclin-dependent kinase inhibitor (p19)	Cell cycle	NM_001800	1.8
TNFRSF14	LIGHT	Immunity and defense	NM_003820	1.8
TNFRSF7	CD27	Immunity and defense	NM_001242	1.8
PPM1B	Protein phosphatase 1B	Signal transduction	NM_002706	1.8
Down-regulated genes				
ADAM19	A disintegrin and metalloproteinase domain 19	Signal transduction	NM_033274	−4.5
ZNF76	Zinc finger protein 76	DNA binding and metabolism	NM_003427	−2.7
RASA1	RAS p21 protein activator 1	Signal transduction	NM_022650	−2.6
HDAC4	HDAC 4	DNA binding and metabolism	NM_006037	−2.4
TXNRD2	Thioredoxin reductase 2	Sulfur metabolism	NM_006440	−2.3
MYC	c-MYC	Apoptosis; proliferation	NM_002467	−2.2
EDG4	Endothelial differentiation GPCR 4	Proliferation; differentiation	AF011466	−2.2
HDAC7A	HDAC 7A	DNA binding and metabolism	NM_016596	−2.2
CHEK1	Chk1 checkpoint homologue 1	Proliferation; differentiation	NM_001274	−2.1
HDAC8	HDAC 8	DNA binding and metabolism	NM_018486	−2.1
CTBP1	COOH-terminal binding protein 1	DNA binding and metabolism	NM_001328	−2.1
DSC3	Desmocollin 3	Cell adhesion	NM_024423	−2.0
CCNT2	Cyclin T2	DNA binding and metabolism	NM_001241	−2.0
ERBB2	HER2/NEU	Signal transduction	NM_004448	−1.9
CCNDBP1	Cyclin D-type binding protein 1	Proliferation and differentiation	NM_012142	−1.8
CDC25C	Cell division cycle 25C	Cell cycle	NM_022809	−1.8

Consistent with the reported biological effects of other HDAC inhibitors, CRA-024781 induced histone and tubulin acetylation, and $p21^{Cip1/WAF1}$ protein, as well as inhibited the growth of 10 human tumor cell lines and nonneoplastic HUVEC *in vitro*. Two cell lines derived from colorectal adenocarcinomas, HCT116 and DLD-1, were further characterized. These two cell lines differ in several respects, including doubling time (see Table 2) and p53 status: HCT116 cells contain wild-type p53, whereas DLD-1 cells express mutant p53 ($Ser^{241}Phe$). Despite these differences, inhibition of cell growth by CRA-024781 *in vitro* was similar in these lines. In both cell lines, growth inhibition was accompanied by changes in several known biomarkers of HDAC response. These biomarkers included the accumulation of acetylated histones and acetylated tubulin. In both tumor cell lines, acetylated tubulin was detectable at lower concentrations than acetylated histones, which might reflect differing sensitivities for specific HDACs or HDAC substrates in the cell, or may reflect differing sensitivities of the specific detection reagents used. Other biomarkers included the accumulation of the tumor suppressor protein $p21^{Cip1/WAF1}$, and the generation of cleaved PARP fragment and phosphorylated H2AX (γH2AX), two known markers of apoptosis. Interestingly, treatment of nonneoplastic HUVEC with CRA-024781 under the same conditions did not lead to PARP accumulation or γH2AX, despite a cellular $GI_{50\%}$ and doubling time in the same range as DLD-1 and HCT116 tumor cells. These data suggest that CRA-024781 may induce apoptosis more effectively or rapidly in tumor cells relative to HUVEC. If generally true in nonneoplastic cells, this observation could partly explain the ability to inhibit tumor growth *in vivo* at dosages that are well tolerated.

CRA-024781 had an *in vivo* pharmacokinetic profile that suggested adequate drug exposure to allow HDAC inhibition *in vivo*. The 10 mg/kg i.v. dose achieved a

plasma concentration above the measured cellular $GI_{50\%}$ for HCT116 tumor cells for 15 minutes. However, it is difficult to predict a priori the *in vivo* drug exposure (area under the curve) that will be adequate for efficacy based on $GI_{50\%}$ or on the appearance of mechanistic biomarkers (protein acetylation, etc.), because these values are based on continuous exposure of tumor cells to the drug *in vitro*, on the other hand, tumors grown *in vivo* are exposed to the drug on a certain schedule (e.g., q.d. × 4 for 16 days) at varying concentrations of compound based on the pharmacokinetics and degree of protein binding of the drug in plasma. Also, the drug concentration in plasma does not necessarily reflect the concentration distributed to the tumor. Indeed, the relatively high steady-state volume of distribution (9,230 mL/kg) suggests that CRA-024781 may readily distribute into tissues. Nevertheless, the doses required for maximal efficacy (≥80 mg/kg) are >10 mg/kg, perhaps because HDAC enzymes must be inhibited for a more prolonged period of time or to a greater extent following each dose in order to achieve antitumor efficacy.

Antitumor activity was shown in two independent colorectal xenograft models, HCT116 and DLD-1. The degree of tumor growth inhibition observed with CRA-024781 is similar to that seen with other published HDAC inhibitors, including trichostatin A (16), LAQ-824 (6, 17), MS-275 (18, 19), PXD101 (20), Cpd 2 (21), cyclic hydroxamic acid containing peptide 31 (22), and Valproate (23). In order to follow the inhibition of HDAC activity over time, we assayed the acetylation of tubulin in blood as a pharmacodynamic marker. The efficacious doses of CRA-024781 delivered to the mice were accompanied by an accumulation of tubulin acetylation in peripheral blood as early as 2 hours after dosing, and levels persisted for at least 6 hours following dosing. Therefore, the kinetics of appearance and disappearance of this biomarker can be used to confirm HDAC inhibition *in vivo*, and may provide a reasonable surrogate marker for clinical monitoring. The acetylation profile in the HCT116 dose-response experiment suggests that in order to achieve robust *in vivo* efficacy, HDACs must be inhibited for a period of 6 hours or longer, because at that time point, the more efficacious doses of 160 and 80 mg/kg resulted in greater accumulation of tubulin than the lower doses, which were not as effective.

CRA-024781 displayed similar inhibition of cell growth and induction of apoptosis in HCT116 and DLD-1 cell lines *in vitro* and inhibited HDACs *in vivo*, as measured by acetylated tubulin in blood, yet the compound seemed to be more inhibitory in the HCT116 xenograft model relative to the DLD-1 model, particularly when the compound was dosed according to the q.d. × 4 per week regimen. The differing sensitivities of HCT116 and DLD-1 xenografts to CRA-024781 *in vivo* may be due to adaptive responses *in vivo* which render DLD-1 less dependent on HDACs for growth and survival.

To investigate the mechanism of action of CRA-024781 *in vivo*, we focused efforts on the analysis of mRNA expression patterns over time in the colorectal xenograft models at doses where efficacy was observed. In the HCT116 xenograft study, a total of 990 genes (or ~15% of the genes analyzed on the array) were found to be differentially expressed by at least 1.8-fold at any time point, and over half of these were down-regulated. This suggests that (*a*) *in vivo*, down-regulation of genes that may be essential for cell proliferation or survival may contribute to the antiproliferative effect of HDAC inhibitors, and (*b*) based on the large number of differentially regulated genes, the antitumor mechanism is likely to be complex. A pattern of similarly up-regulated genes was observed 2 hours following dosing at 80 mg/kg (HCT-116) and 160 mg/kg (DLD-1; Fig. 6, *red box*). Interestingly, the up-regulated (*red box*) genes were not observed at 2 hours in the sensitive HCT-116 tumors treated at the highest dose of 160 mg/kg, consistent with a more rapid onset of events under these conditions. At later (4- to 6-hour) time points, the dominant pattern is a set of genes that become down-regulated (*yellow box*). Therefore, it seems that an early pattern of genes is induced within 2 hours followed by a later pattern of down-regulated genes at 4 to 6 hours.

A selection of genes with at least 1.8-fold differential expression ($P < 0.05$) averaged over the early and mid time points is shown in Table 3. The list includes genes with the highest fold change that also have a known biological function, and specifically includes many genes that have previously been shown to be regulated by HDAC inhibitors such as suberoylanilide hydroxamic acid and trichostatin A (4), for example, $p21^{Cip1/WAF1}$ (CDKN1A) and caspases (CASP1, CASP3), as well as TNFR superfamily members including TNFRSF 7 (CD27) and 14 (LIGHT), as well as serpins, and a histone subunit. The up-regulated pattern is consistent with the induction of apoptosis being one of the mechanisms of action of this compound. Down-regulated genes include cyclins and other cell division control proteins, several HDACs, c-MYC, and Her2/NEU (ERBB2). The down-regulation of several HDAC isoforms suggests the presence of transcriptional feedback loops resulting from HDAC inhibition, which may result in prolonging the re-expression of genes. The observation that the prominent down-regulated genes include MYC, cyclins, and other proteins required for cell division, and that the cyclin inhibitor $p21^{Cip1/WAF1}$ is up-regulated, suggests that cell cycle arrest leading to reduced proliferation is an important part of the mechanism of tumor growth inhibition *in vivo*, in agreement with previous *in vitro* observations (21, 24). Thus, growth arrest and apoptosis in both HCT116 and DLD-1 tumors could occur in part by up-regulating $p21^{Cip1/WAF1}$ to induce arrest in G_1 and apoptosis. In addition, the tumor suppressor p19 (INK4d), a gene previously shown to be an important mechanism of growth arrest in HCT116 cells *in vitro* (25), is also up-regulated in these tumors.

In summary, we have identified a novel inhibitor of HDAC, CRA-024781, with antitumor activity *in vitro* and *in vivo*. The results presented here show that CRA-024781 inhibits HDAC enzymes and has antitumor properties *in vivo* at doses that are well tolerated and may therefore be active in a clinical setting in patients with cancer.

Antitumor activity without associated toxicity has been reported for other HDAC inhibitors as well (20, 26, 27). Based on these results, CRA-024781 has entered phase I clinical trials in cancer to determine its safety in humans and suitability for further development as a novel oncolytic agent.

Acknowledgments

We thank the following people for their efforts in the development of CRA-024781: Shawn Misialek, Gail Siu, Joyce Mordenti, Jack Davis, Ling Leung, Anthony Neri; and the following for help in statistical analysis: Ping Zhan and Ondine Callan.

References

1. De Ruijter AJM, van Gennip AH, Caron HN, Kemp S, van Kuilenburg ABP. Histone deacetylases (HDACs): characterization of the classical HDAC family. Biochem J 2003;370:737 – 49.

2. Buggy JJ, Sideris ML, Mak P, Lorimer DD, McIntosh B, Clark JM. Cloning and characterization of a novel human histone deacetylase, HDAC8. Biochem J 2000;350:199 – 205.

3. Matsuyama A, Shimazu T, Sumida Y, et al. *In vivo* destabilization of dynamic microtubules by HDAC6-mediated deacetylation. EMBO J 2002; 21:6820 – 31.

4. Drummond DC, Noble CO, Kirpotin DB, Guo Z, Scott GK, Benz CC. Clinical development of histone deacetylase inhibitors as anticancer agents. Annu Rev Pharmacol Toxicol 2004;45:495 – 528.

5. Fraga MF, Ballestar E, Villar-Garea A, et al. Loss of acetylation at Lys16 and trimethylation at Lys20 of histone H4 is a common hallmark of human cancer. Nat Genet 2005;37:391 – 400.

6. Qian DZ, Wang X, Kachhap SK, et al. The histone deacetylase inhibitor NVP-LAQ824 inhibits angiogenesis and has a greater antitumor effect in combination with the vascular endothelial growth factor receptor tyrosine kinase inhibitor PTK787/ZK222584. Cancer Res 2004;64:6626 – 34.

7. Maison C, Bailly D, Peters A, et al. Higher-order structure in pericentric heterochromatin involves a distinct pattern of histone modification and an RNA component. Nat Genet 2002;30:329 – 34.

8. Cimini D, Mattiuzzo M, Torosantucci L, Degrassi F. Histone hyper-acetylation in mitosis prevents sister chromatid separation and produces chromosome defects. Mol Biol Cell 2003;14:3821 – 33.

9. Miller TA, Witter DJ, Belvedere S. Histone deacetylase inhibitors. J Med Chem 2003;46:5097 – 116.

10. Cao ZA, Bass KE, Neri A, et al. Characterization of CRA-024781, a potent histone deacetylase inhibitor, as a cancer therapeutic. Proc Am Assoc Cancer Res 2005;46:422.

11. Schultz BE, Misialek S, Wu J, et al. Kinetics and comparative reactivity of human class I and class IIb histone deacetylases. Biochemistry 2004;43:11083 – 91.

12. Kuzmic P, Elrod KC, Cregar LM, Sideris S, Rai R, Janc JW. High-throughput screening of enzyme inhibitors: simultaneous determination of tight-binding inhibition constants and enzyme concentrations. Anal Biochem 2000;286:45 – 50.

13. de Fries R, Mitsuhashi M. Quantification of mitogen induced lymphocyte proliferation: comparison of Alamar blue assay to ^{3}H-thymidine incorporation assay. J Clin Invest 1995;9:89 – 95.

14. Archer SY, Meng S, Shei A, Hodin RA. p21(WAF1) is required for butyrate-mediated growth inhibition of human colon cancer cells. Proc Natl Acad Sci U S A 1998;95:6791 – 6.

15. Rogakou EP, Nieves-Neira W, Boon C, Pommier Y, Bonner WM. Initiation of DNA fragmentation during apoptosis induces phosphorylation of H2AX histone at serine 139. J Biol Chem 2000;275:9390 – 5.

16. Touma SE, Goldberg JS, Moench P, et al. Retinoic acid and the histone deacetylase inhibitor trichostatin a inhibit the proliferation of human renal cell carcinoma in a xenograft tumor model. Clin Cancer Res 2005;11:3558 – 66.

17. Drummond DC, Marx C, Guo Z, et al. Enhanced pharmacodynamic and antitumor properties of a histone deacetylase inhibitor encapsulated in liposomes or ErbB2-targeted immunoliposomes. Clin Cancer Res 2005;11: 3392 – 401.

18. Camphausen K, Scott T, Sproull M, Tofilon PJ. Enhancement of xenograft tumor radiosensitivity by the histone deacetylase inhibitor MS-275 and correlation with histone hyperacetylation. Clin Cancer Res 2004; 10:6066 – 71.

19. Saito A, Yamashita T, Mariko Y, et al. A synthetic inhibitor of histone deacetylase, MS-27 – 275, with marked *in vivo* antitumor activity against human tumors. Proc Natl Acad Sci U S A 1999;96:4592 – 7.

20. Plumb JA, Finn PW, Williams RJ, et al. Pharmacodynamic response and inhibition of growth of human tumor xenografts by the novel histone deacetylase inhibitor PXD101. Mol Cancer Ther 2003;2:721 – 8.

21. Fournel M, Trachy-Bourget MC, Yan PT, et al. Sulfonamide anilides, a novel class of histone deacetylase inhibitors, are antiproliferative against human tumors. Cancer Res 2002;62:4325 – 30.

22. Komatsu Y, Tomizaki KY, Tsukamoto M, et al. Cyclic hydroxamic-acid-containing peptide 31, a potent synthetic histone deacetylase inhibitor with antitumor activity. Cancer Res 2001;61:4459 – 66.

23. Takai N, Desmond JC, Kumagai T, et al. Histone deacetylase inhibitors have a profound antigrowth activity in endometrial cancer cells. Clin Cancer Res 2004;10:1141 – 9.

24. Peart MJ, Smyth GK, van Laar RK, et al. Identification and functional significance of genes regulated by structurally different histone deacetylase inhibitors. Proc Natl Acad Sci U S A 2005;102:3697 – 702.

25. Yokota T, Matsuzaki Y, Miyazawa K, Zindy F, Roussel MF, Sakai T. Histone deacetylase inhibitors activate INK4d gene through Sp1 site in its promoter. Oncogene 2004;23:5340 – 9.

26. Butler LM, Agus DB, Scher HI, et al. Suberoylanilide hydroxamic acid, an inhibitor of histone deacetylase, suppresses the growth of prostate cancer cells *in vitro* and *in vivo*. Cancer Res 2000;60: 5165 – 70.

27. Saito A, Yamashita T, Mariko Y, et al. A synthetic inhibitor of histone deacetylase, MS-27-275, with marked *in vivo* antitumor activity against human tumours. Proc Natl Acad Sci U S A 1999;96: 4592 – 7.